Solar Energy 207 (2020) 1214–1221

Contents lists available at ScienceDirect

Solar Energy

journal homepage: www.elsevier.com/locate/solener

Solar vapor generation using bubbly flow nanofluids with collaborative light-harvesting nanoparticles

Guansheng Yao[a], Yijun Feng[a], Guohua Liu[a,b,*], Jinliang Xu[a,b]

[a] Beijing Key Laboratory of Multiphase Flow and Heat Transfer for Low Grade Energy Utilization, North China Electric Power University, Beijing 102206, PR China
[b] Key Laboratory of Power Station Energy Transfer Conversion and System (North China Electric Power University), Ministry of Education, Beijing 102206, China

ARTICLE INFO

Keywords:
Solar evaporation
Nanofluid
Bubble
Plasmonic heating
Vapor generation

ABSTRACT

Nanotechnology can produce metallic particles of nanometer sizes with unique optical and thermal properties. Utilizing the nanofluid in solar systems has distinct advantages over conventional fluids in light harvesting, thermal generation and heat transport. However, the plasmonic effect only induces strong light absorption around its nature resonance peak, which is not desirable for broadband solar absorption. Herein, we propose a composite nanofluid composed of three different kinds of particles with distinguish absorbance peaks for collaborative light absorption over the entire solar spectrum. Dynamic bubbles are further introduced into the nanofluid to promote the solar vapor generation. With light absorption spanning from ultraviolet, visible to near-infrared wavelengths, these particle-bubble couplings induce multiple scattering events, increasing photon absorption and light flux within local domain, leading to intensive heating that activates phase-change evaporation in the close proximity. The bubbly flow nanofluid exhibits the best photothermal efficiency of 91.2% than that of the other counterparts, enabling fast vapor diffusion with an upward bubble-bursting flow, and therefore achieving a decent steam generation efficiency of 40.8% under one-sun irradiation. Our findings not only suggest a new way to improve solar vapor generation in laden-particle solution, but also shed lights on the development of novel solar thermal systems.

1. Introduction

As the primary energy source for the earth, solar energy harvesting and conversion is critical important for development of renewable energy. Within this framework, direct absorption of solar energy by use of the working fluids has great practicability in reducing the heat loss and improving the thermal conversion efficiency (Gao et al., 2019; Shin et al., 2018; Tao et al., 2018). Diverse working fluids have been studied by seeding the solution with particles such as carbon-based materials or graphite (Chen et al., 2019; Loeb et al., 2018; Ni et al., 2015), metallic nanostructures, titanium and copper oxide, etc. (Liu et al., 2017a; Qu et al., 2019; Zeng et al., 2016). Among them, plasmonic nanofluids attract more attention to other fluids owing to their tunable optical properties with strong response to visible light, which is beneficial for solar absorption (Zhou et al., 2017; Ni et al., 2015; Neumann et al., 2013). The overlapping between the incident light frequency and the resonance frequency of metals would induce intensive oscillations of free electrons over the whole particle due to the plasmonic resonance effect, which leads to energy decay of the hot electrons (Govorov and Richardson, 2007; Liu et al., 2017b), and thus a considerable increasing of temperature of the metallic structures as well as the surrounding environment can be observed (Jauffred et al., 2019; Liang et al., 2019).

Au plasmonic nanofluids have been most studied for solar thermal conversion due to its excellent light-to-heat converting efficiency with a thermal efficiency above 24% (Liu et al., 2017b; Amjad et al., 2017; Wang et al., 2017). While the fluid has intrinsic limitation of a narrow bandwidth enhancement of light absorption, which restricts a broadband-light harvesting of solar energy (Hedayati et al., 2012; Liang et al., 2019). Various methods have been proposed to improve the performance (Bermel et al., 2016; Huiling Duan, 2017; Li et al., 2020). Hybridizing Au structures with different morphologies such as nanoparticles, nanorods, and nanostars can effectively optimized interactions between the incident light and nanostructures that greatly extends the absorption spectrum (Jeon et al., 2014; Jiang et al., 2018; Du and Tang, 2016). However, the high cost of Au is not feasible for practical application (Zeiny et al., 2018). Blending metal particles with other dielectric materials is another alternative to tune the absorption band (Jeon et al., 2016; Ross et al., 2014; Verma et al., 2018). For

* Corresponding author at: Beijing Key Laboratory of Multiphase Flow and Heat Transfer for Low Grade Energy Utilization, North China Electric Power University, Beijing 102206, PR China.
E-mail address: liuguohua126@126.com (G. Liu).

https://doi.org/10.1016/j.solener.2020.07.057
Received 25 May 2020; Received in revised form 1 July 2020; Accepted 17 July 2020
Available online 24 July 2020

Nomenclature

c	specific heat capacity of water
e	electronic charge
h_{fg}	latent heat of vaporization
$m1$	total mass of solution
Me	electronic mass
$meva$	vapor mass flux
N	electron concentration
$Qsolar$	total incoming solar flux
S	heating area
T	evaporation duration

Greek symbols

ΔT	temperature increasing of liquid
ε_0	dielectric constant of vacuum
ω_p	plasmon frequency
ν	steam generation rate
$\eta_{evaporation}$	evaporation efficiency
$\eta_{heating}$	heating efficiency of liquid
$\eta_{photothermal}$	total photothermal efficiency

example, Halas et al. dispersed a core-shell structure of SiO_2/Au nanoparticles in liquid to improve solar vapor generation (Neumann et al., 2013), resulting in an obviously red-shifted resonance with roughly overlapping of solar spectrum. Although some studies are beneficial to the full spectrum absorption of solar energy, the complex and reliable preparation of photothermal materials remain challenging.

The photothermal conversion process is not only dependent on the light absorption and heat generation, but also closely related to vapor diffuse at the interface (Chen et al., 2017; Ma et al., 2018; Zhou et al., 2016). Halas et al. calculated the electric field distribution in high-concentration Au nanofluids and found that the multiple internal scattering of particles can significantly increase the optical path, and enhance the light-to-heat conversion (Hogan et al., 2014). But high concentrations of nanofluids are expansive and not suitable for large-scale application. In contrast to volumetric heating system, various photothermal sheets aiming to minimize the heat loss are also used in solar water evaporation. These photothermal sheets placed on the water surface can effectively inhibit the thermal losses caused by radiation, convection and ineffective heat conduction while improving photon capture, so that most of the absorbed solar energy is converted into enthalpy change in the process of water evaporation, greatly improving the energy conversion efficiency. However, such interfacial absorbing system require elaborates design of structures and systems. Recently, we proposed a new way to accelerate the steam generation by coupling bubbles within the plasmonic nanofluids (Yao et al., 2020). The bubble-nanofluid couplings significantly improve the light harvesting, heat and mass transfer as well as the vapor diffusion process, resulting in a three-time enhancement of the evaporation rate of pure water.

In this work, we verify the solar vapor generation using bubbly flow nanofluids with broadband-light harvesting nanoparticles. With the concept, a hybrid nanofluid composed of three different kinds of nanoparticles (TiO_2, Au and Indium tin oxide (ITO)) with distinguish absorbance peaks are prepared for collaborative light absorption ranging from ultraviolet, visible to infrared regime (see Fig. 1). The intrinsic resonance frequencies of single nanofluid of TiO_2, Au and Indium tin oxide lies in the ultraviolet, visible and infrared regions, respectively. Dynamic bubbles are then introduced into the hybrid nanofluid to further improve the vapor generation. These particle-bubble couplings induce multiple scattering events, increasing photon absorption and light flux within local domain, leading to intensive heating with a prominent vapor generation efficiency of 40.8% under one-sun irradiation. Utilization of the composite nanofluids is not limited to solar desalination applications, but also can be extended into the energy storage and power generation process.

2. Experimental section

The diagram of the experimental setup is shown in Fig. 2. A solar simulator (CEL-PE300-3A) was employed as light source, which matches with the AM1.5 spectrum well. An electronic balance (Precisa LS/LT/LX 620 M, 0.1 mg accuracy) connected to computer was used to record the mass change of solution. A porous metal sinter is utilized to create bubbles flowing into the glass container (40 mm × 100 mm). An experiment fluid of 100 ml (~80 mm depth) was added into the glass container. A gas cylinder supplies the pressured air into the porous sinter to generate bubbles. A needle valve and a rotameter were used to control the air flow rate. In this experiment, the gas flow rate was set at 20 ml/min. K-type thermocouples were embedded in the glass column to trace the temperatures (T_1, T_2, T_3). The distance between three thermocouples was set at 35 mm to measure the temperature of upper, middle and bottom of working liquids, respectively. The temperature data were recorded per second by a data acquisition model (Agilent 34970A). An infrared camera (IR 5300 Series, Germany) was adopted to record the water surface temperature at frequency of 1 Hz. A high-speed camera (IDT Motion Pro Y4, USA) was installed for recording the evolution of flow-pattern with frequency of 1000 Hz. The solar intensity was maintained at 1 kW/m^2 at an ambient temperature of 25 °C.

Au nanofluids are synthesized by the citrate reduction method (Liu et al., 2018). While TiO_2 and ITO nanofluids are purchased from Huzheng nano-science company in Shanghai and used as received. The composite nanofluids was diluted drop by drop in DI water under stirring with a speed of 300 rpm. The resulting mixture was stirred for 20 min. The composite nanofluid is composed of 50 ppm of Au, 1000 ppm of TiO_2 and 1000 ppm of ITO with similar magnitude for light absorption. Semi-quantitative chemical composition detection (EDS) and morphology analysis of hybrid nanofluids was performed on

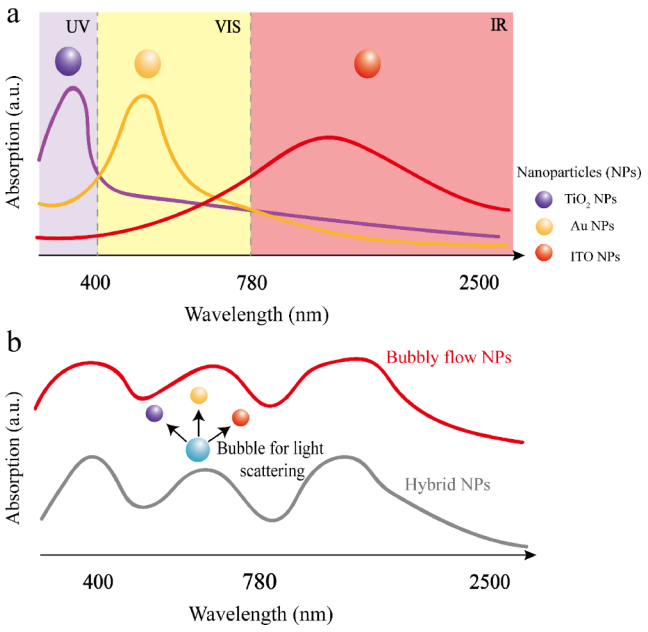

Fig. 1. Conceptual design of the bubbly flow nanofluids with broadband-light harvesting nanoparticles, (a) different nanoparticles for light harvesting with distinct absorption peaks, (b) the enhanced absorption induced by light scattering effect of bubbles.

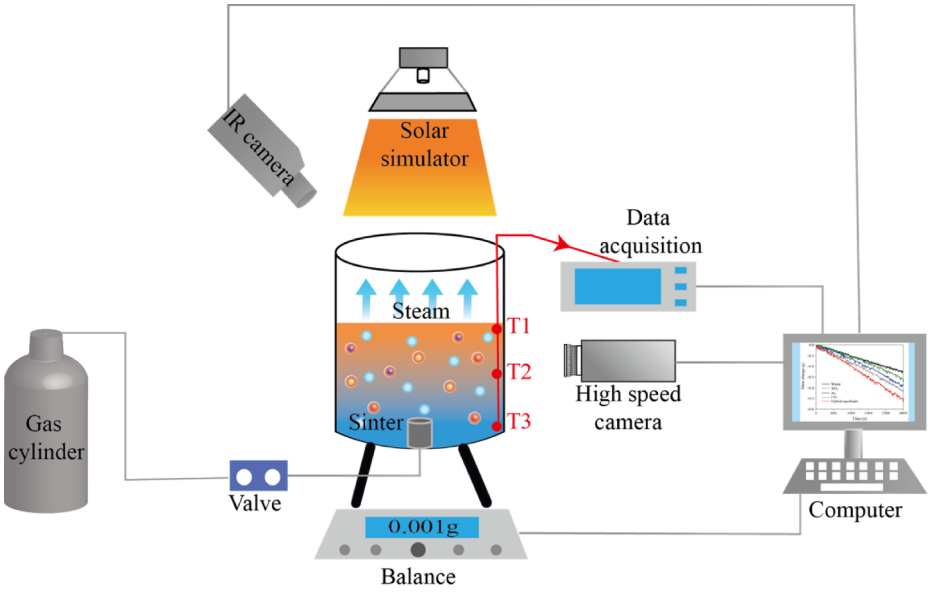

Fig. 2. The experimental setup.

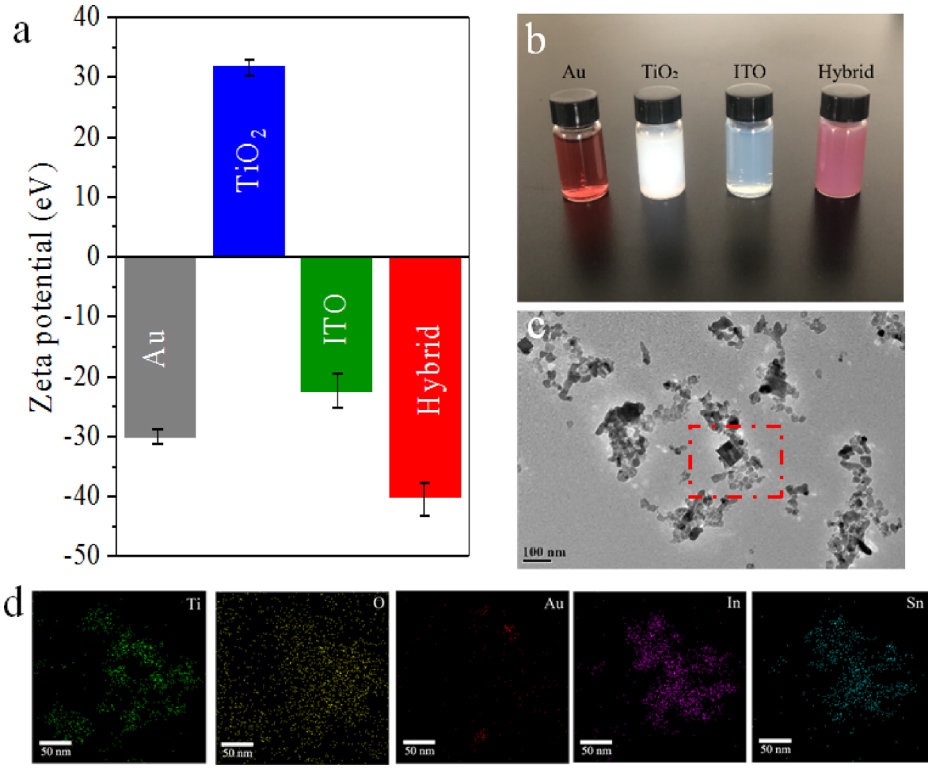

Fig. 3. (a) Zeta-potential of the nanofluids, (b) A photo of the nanofluids: Au, TiO_2, ITO and composite nanofluid, (c) a TEM image of the composite nanofluid, and (d) the corresponding EDX elemental mapping.

a JFM-2100F transmission electron microscope operating at a bias voltage of 200 kV. A UV–Visible-NIR-Spectrophotometer (Lambda 750, PerkinElmer, USA) was used to measure the absorption property range 280 nm from 1400 nm and the DI water was used as comparison standards. Zeta potential of these nanofluids were tested by a Zetasizer Ultra (Malvern Panalytical) to determine the stability of the nanofluids.

Zeta potentials of the nanofluids are indicated in Fig. 3a, showing good stability of all the solutions. The composite nanofluid with a negative potential peak of −40.1 mV demonstrates the best stability than the other nanofluids. Fig. 3b presents an image of the corresponding nanofluids with an obviously colorful difference of the solutions. The high-resolution TEM image (Fig. 3c) shows the excellent dispersion and quasi-spherical morphology of the nanoparticles. The element distribution maps of the composite are shown in Fig. 3d, which confirms the co-existence of Ti, O, Au, In and Sn components that they are heterogeneously dispersed in the solution. When these nanoparticles close package to each other, the coupling effect by subtle distribution of these particles will induce plasmonic Fano resonance, which is advantages for broadening light absorption (Jauffred et al., 2019; Jiang et al., 2018).

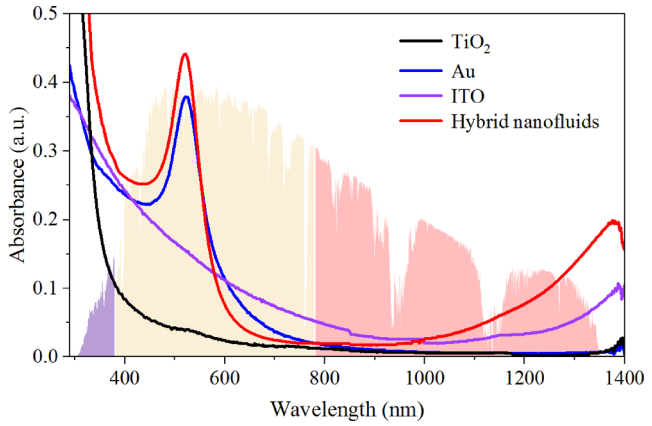

Fig. 4. Absorption spectrum of the TiO_2, Au, ITO and composite nanofluids (The colored shaded portion of the background represents the intensity of the solar spectrum with purple, orange and pink color corresponding to the UV, visible and IR region, respectively). (For interpretation of the references to color in this figure legend, the reader is referred to the web version of this article.)

3. Results and discussion

The optical absorption spectra of the nanofluids are presented in Fig. 4. The relationship between plasmon frequency ω_p and electron concentration can be described by the Mott-Smith equation:

$$\omega_p = \sqrt{4\pi n e^2 / m_e \varepsilon_0} \quad (1)$$

where n is electron concentration, ε_0 is dielectric constant of vacuum, e is electronic charge and m_e is electronic mass (Langmuir, 1928). Au nanofluids have a high electron concentration with a distinct absorption peak at about 520 nm due to the local surface plasmon resonance (Link and El-Sayed, 1999). The TiO_2 nanofluids exhibits strong absorption below the 400 nm wavelengths, while the electron concentration of ITO is very low and it's oscillation frequency is in the infrared band (Franzen, 2002). Therefore, the absorption spectra of the composite nanofluids can be flexibly tuned by changing the composed solution. The composite nanofluids thus shows a desirable broad-band light absorption spanning from ultraviolet, visible to near-infrared wavelengths, which is beneficial for solar energy harvesting (Hedayati et al., 2012).

Based on the prepared nanofluids with broad-band light harvesting properties, dynamic air bubbles are introduced into the nanofluids to study the solar vapor generation process. Fig. 5 gives the typical flow-pattern of different nanofluids. The behavior of rising bubbles is complex that depends on its size and shape, operating temperature and properties of the solution. The thermal radiation not only changes the liquid temperature and viscosity, but also introduces all known non-Newtonian phenomena. A smaller bubble size with a better dispersion in the column evaporator is observed compared with that of the bubbly flow. There many forces acting on the bubbles that the rising path is not straight up. In its rising process, they collide with the surrounding nanoparticles, which not only impacts its temperature and viscosity but also induces the elastic shear deformation. Hereby, the motion of dispersed bubbles is accompanied by a combination of trajectory oscillations and shape deformation oscillations at a limited rise velocity. The high-speed bubbly flow between gas and liquid finally causes bubble bursting at air/water interface, which greatly promote the vapor diffusion process. Besides, during the rising process of dynamic bubbles, the unstable interfaces between gas and liquid phases enhance the mass transfer for moisture absorption (Fan et al., 2014), thus significantly improving the humidity of air bubbles. The steam then is released into the air after the bubble bursting, which further promotes vapor diffusion with a fluctuation interface (Abd-ur-Rehman and Al-Sulaiman, 2017).

The transient surface temperature of working fluid is shown in Fig. 6a–b. It can be seen that the composite nanofluid has the highest temperature in all the cases, approaching to 35 °C after one-hour solar illumination. However, after air bubbles injection into nanofluids, the temperature is lowest at the gas-liquid interface among the different nanofluids. This sharp contrast change comes from the thermal balance from two aspects: (1) the composite nanofluid harvests broad spectrum wavelengths of solar energy, signifying more light absorption and photothermal production from the plasmonic effect. (2) Although the light scattering nature of bubbles increase the light flux, the bubbly flow takes away more thermal energy for phase change evaporation of the proximity liquid, thus leading to less thermal energy for sensible heating of the fluid. Fig. 6c and d present vertical temperature distribution of the nanofluids and bubbly flow case, respectively. The large temperature gradient presents in the composite nanofluids, while a nearly uniform temperature of the bubbly flow is observed as a fast thermal equilibrium can be achieved due to the induced turbulence flow around bubbles. Fig. 7 shows the instantaneous thermal images captured by the infrared camera. It is found that the composite nanofluids near the container are hotter than those in the middle, because a large vapor flux can be expected in center region. As for the bubbly flow nanofluids, the bubble spray process at the air-liquid interface induces small temperature oscillation ~2 °C at liquid interfaces. The temperature of the bursting droplet is highest over the whole interface of water that will drive fast evaporation of the small droplet with an extend duration, which is thus advantage for more vapor generation (Yao et al., 2020).

Fig. 8 presents the vapor generation performance under one-sun. It can be seen that all the nanofluids enhance the vapor generation process. The maximum error of mass loss evaluated from our experiments is below 6.5%. Interestingly, with the adding Au nanoparticles into the working fluids, the nanofluid shows a better vapor production performance, a water loss of 0.45 g compared to that of pure water ~0.22 g

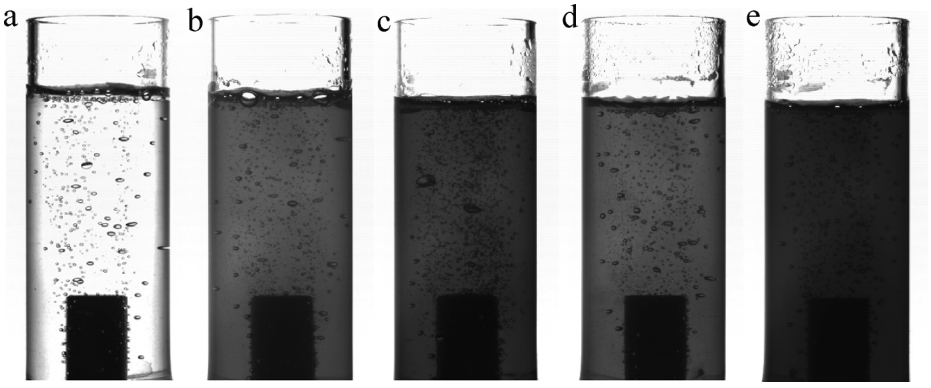

Fig. 5. Typical flow-patterns of the bubbly flow nanofluids (a) water, (b) TiO_2, (c) Au, (d) ITO and (e) composite solution.

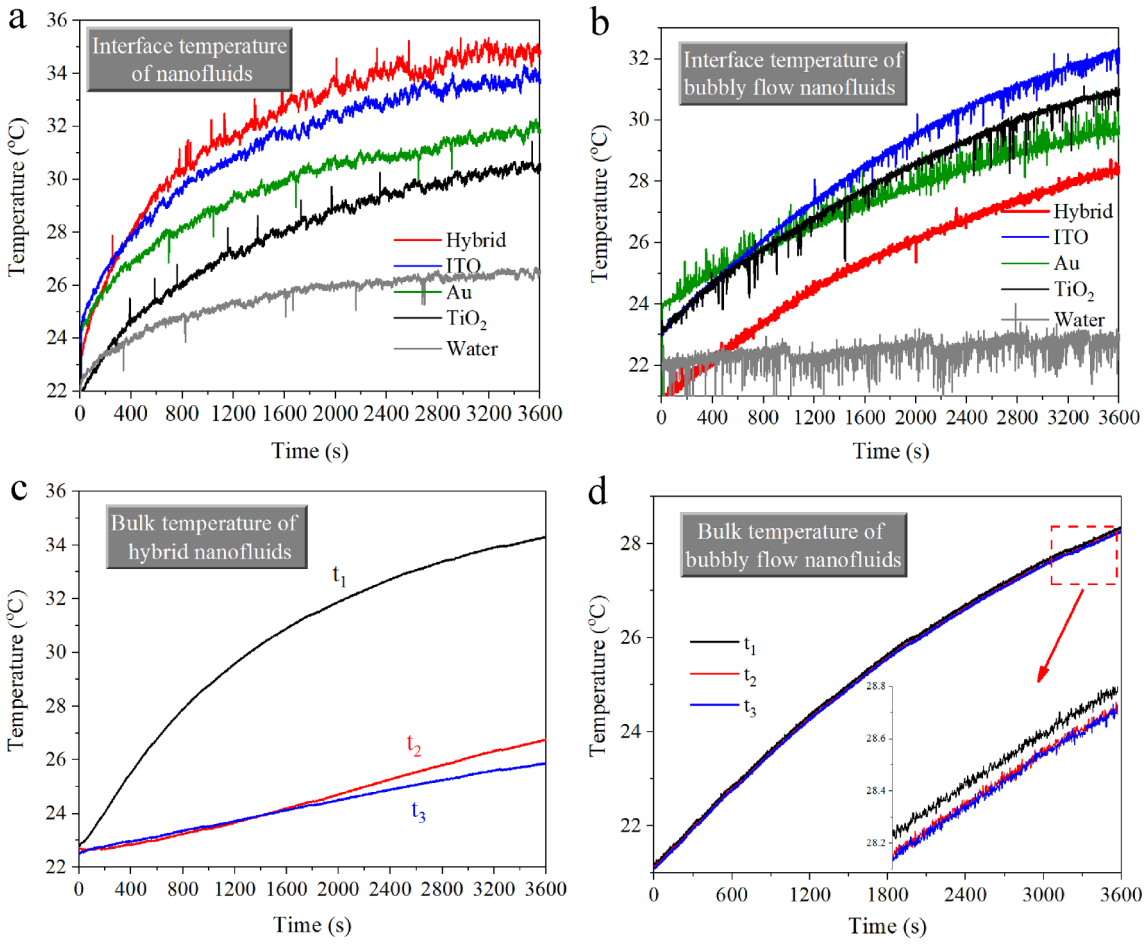

Fig. 6. Evolution of interfacial temperature in solar evaporation of (a) water, TiO_2, Au, ITO and composite nanofluids and (b) bubbly flow nanofluids. Temperature distribution along the column depth with (c) composite nanofluid and (d) bubbly flow nanofluid.

(Fig. 8a). In addition, owing to the coupling effect between bubbles and nanoparticles, a larger water loss of 0.89 g is further achieved with addition of the dynamic bubbles (Fig. 8b). Fig. 8c shows the evaporation rate of all tests that is calculated from the mass change over time.

$$\nu = m_{eva}/(T * S) \quad (2)$$

where ν is the steam generation rate (kg $m^{-2}h^{-1}$), m_{eva} is the mass change of base liquid (kg), T is the evaporation duration (h), S is the heating area (m^2). It reflects that introducing bubbles into the composite nanofluid can further improve the steam generation. An appreciable evaporation rate of 0.65 kg $m^{-2}h^{-1}$ can be achieved, which is 3.61 times higher than the pristine water 0.18 kg $m^{-2}h^{-1}$. This performance can be attributed to the broad spectrum light harvesting of the nanofluids and the bursting release of vapor.

Furthermore, we calculate the evaporation efficiency, heating efficiency and total photothermal efficiency of working fluids to quantify the performance of solar steam generation process and highlight the advantages of our concept (Fig. 9). These corresponding efficiencies are defined as

$$\eta_{evaporation} = h_{fg} * \nu/Q_{solar} \quad (3)$$

$$\eta_{heating} = (cm_1\Delta T + m_{eva} * h_{fg})/Q_{solar} \quad (4)$$

$$\eta_{photothermal} = \eta_{evaporation} + \eta_{heating} \quad (5)$$

where $\eta_{evaporation}$, $\eta_{heating}$ and $\eta_{photothermal}$ are the evaporation efficiency, heating efficiency of base liquid and the total photothermal conversion efficiency, respectively. Q_{solar} is the incoming solar flux (1 kw/m^2), h_{fg} is the latent heat of water at 1 atm ($\approx 2.26 \times 10^6$ J kg^{-1}), c is the specific heat capacity of water (4.2×10^3 J kg^{-1} °C^{-1}), m_l is the total mass of solution (kg), ΔT is the temperature increasing of base liquid (°C). (Yao et al., 2020). For the case of pure water, the evaporation efficiency and heating efficiency are 11.3% and 18.8%, respectively, while the composite nanofluid is more efficient in both vapor production and sensible heating of the working fluid, with the corresponding efficiency of 23.2% and 43.5%. For the bubbly flow nanofluids with broadband-light harvesting nanoparticles, the bubbly air flow takes away more heat than its counterpart, and thus demonstrating a reduced heating efficiency. However, the evaporation efficiency increases obviously with a highest photothermal efficiency of 91.6%, which can be attributed to collaborative light absorption of the composed nanoparticles and fast vapor diffusion from the bubble-bursting air flow.

Plasmonic heating effect has been extensively explored over the past decade. However, the full potential of plasmonic structures has not yet been fully exploited, particularly with the addition of new components for realizing multicomponent particles that may lead to improved properties. Here, we demonstrate the composite nanofluid as a typical example of this case that composed of three condensed nanoscale domains with distinctive material compositions or sizes. The nanofluids are the combinations of particles and base water. The nanoparticles enhance the optical and thermal properties of solution, while water strongly absorbs infrared radiation. It is desirable to understand the local heating of individual particles and the global heating of the solution with a certain density of particles. Although the Mie theory provides exact solution on scattering and absorption of sphere-like particles comparable to the light wavelength, it is still challenge to

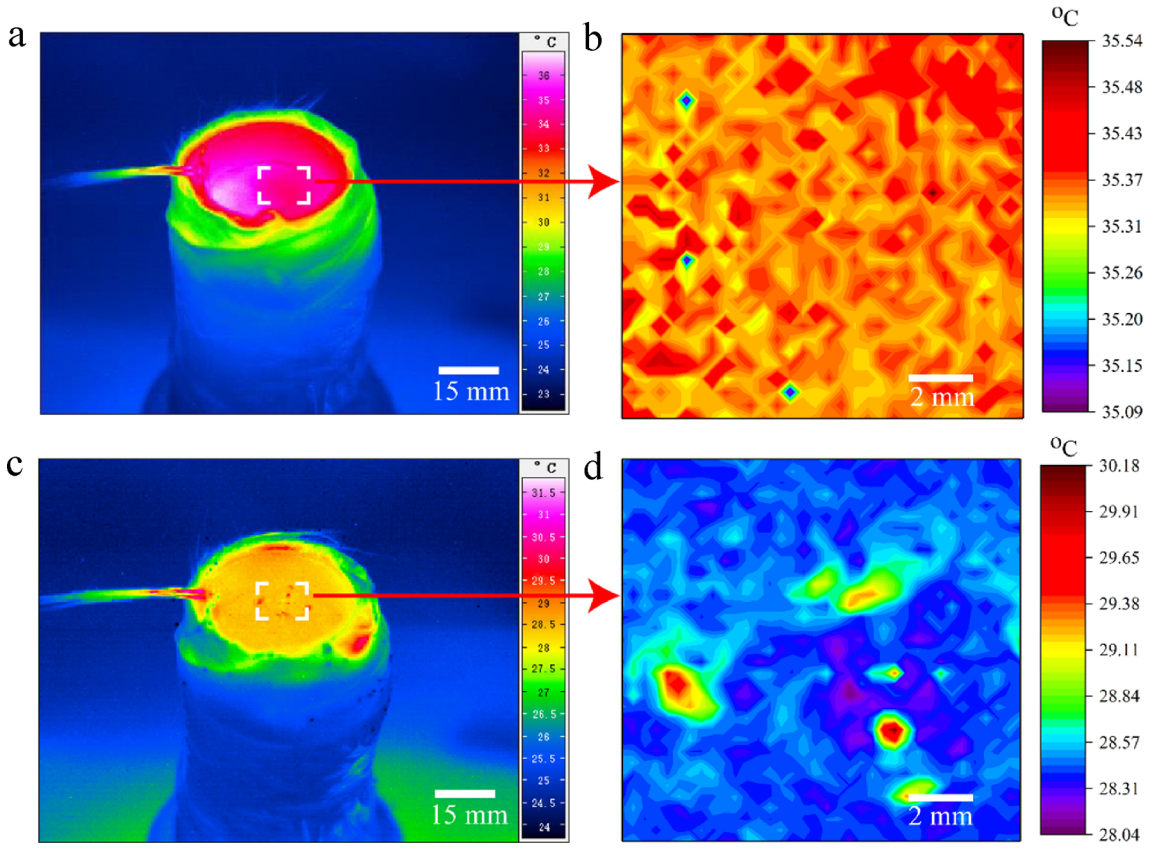

Fig. 7. The infrared camera images of (a) composite nanofluid and (c) bubbly flow nanofluids after one-hour irradiation, (b) and (d) are the temporal oscillations of temperature at air-water interface.

experimentally detect local temperature around particles (Berry et al., 2015; Wang et al., 2019; Yan et al., 2018). To study the photothermal heating transition from a single particle to the bulk solution, we perform temperature measurements over the plasmonic arrays with different spacings in the solution, which may be a bridge between the single particle heating and the collective thermal performance of nanoparticle arrays. Nevertheless, in such a complex geometry, the plasmon hybridization modes in terms of interactions between the plasmon resonances of its elementary components would be induced via the symmetry-broken structures (Ha et al., 2019; Halas et al., 2011). Hereby, there are still opportunities to find new physical mechanisms for improved photothermal performance from the fundamental aspect.

4. Conclusion

The harvesting of renewable solar energy for vapor generation from water offers a potential route for seawater desalination and wastewater treatment. The solar thermal collector using bubbly flow nanofluids with broadband-light harvesting nanoparticles are able to address key challenges such as low light harvesting capability and limited phase-change rate faced in conventional device. Our results reveal that the pronounced broadband absorption properties of nanofluids coupling with the strong scattering of bubbles resulting in a high evaporation efficiency of 40.8%, which is about 3.6-fold enhancement compared with the base water. The overall photothermic efficiency of solar collector is approaching to 92%, indicating such technology is promising for application in solar thermal engineering. The advantages of this concept can be drawn as: (1) the composite nanofluids overcome the inherent defects of narrow-band absorption and possess the wide-band absorption ability for collaborative light absorption over the entire solar spectrum. (2) The dynamic bubbles not only amplify the solar flux via its light scattering nature, but also promote vapor diffusion with an upward bubble-bursting flow. (3) The particle-bubble couplings increase photon absorption and light flux within small local domain, creating intense heating to drive phase-change evaporation. It is expected that the strategy reported here could offer an innovative method for developing high-performance solar collectors or solar steam devices.

To realize the dream of using nanofluid in bubble column evaporator for solar vapor generation, some challenges regarding its theoretical research and practical engineering still require further investigation. For example, the particle-bubble interaction is very complex, it is still difficult to precisely descript the thermal dynamics at air-liquid interface. Moreover, the large-scale engineering applications of seawater desalination must look for materials that are more economical and durable with long-term working stability. In addition, to utilize as much solar energy as possible, well-matched solar spectrum absorbers are highly desirable for further improvement its performance. Obviously, there is still a long way to go, while the physical novelty of the proposed concept makes it promising for solar thermal applications.

Declaration of Competing Interest

The authors declare that they have no known competing financial interests or personal relationships that could have appeared to influence the work reported in this paper.

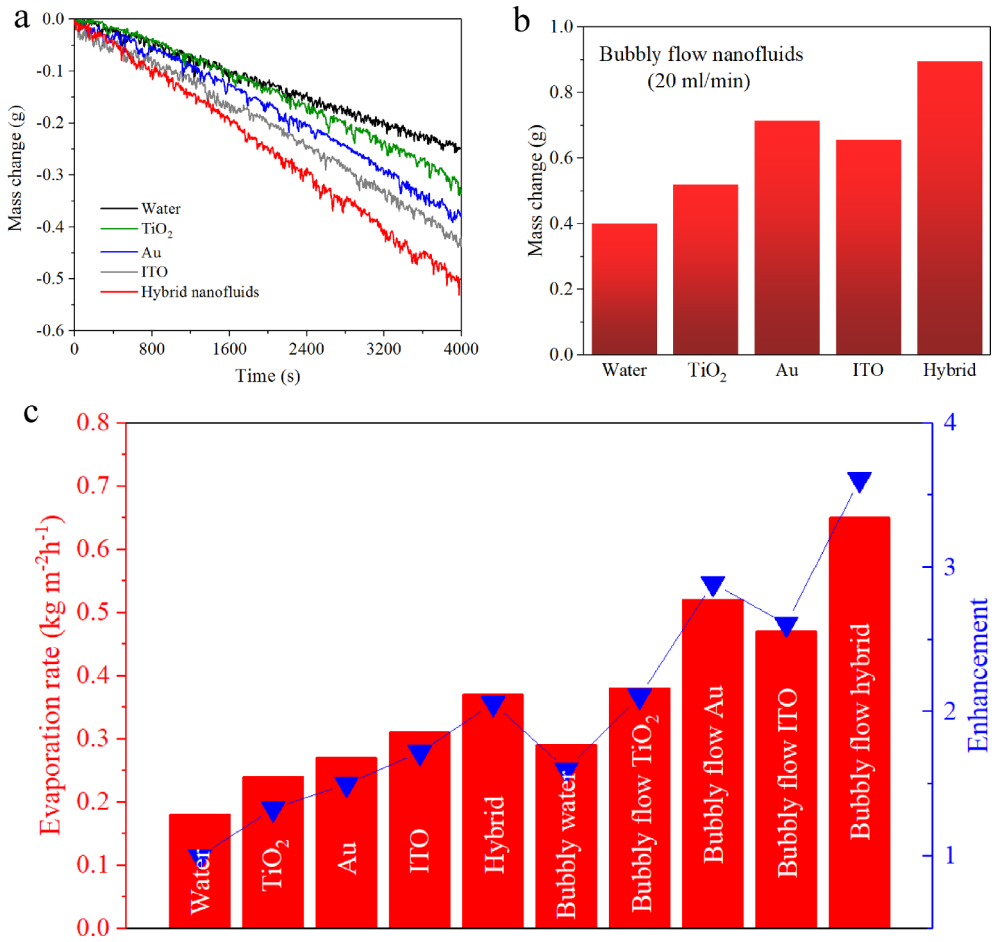

Fig. 8. The performance of solar steam generation. (a) Mass change of different types of nanofluids versus time, (b) the total mass change of bubbly flow nanofluids after 4000 s, and (c) the corresponding evaporation rates and enhancement ratios.

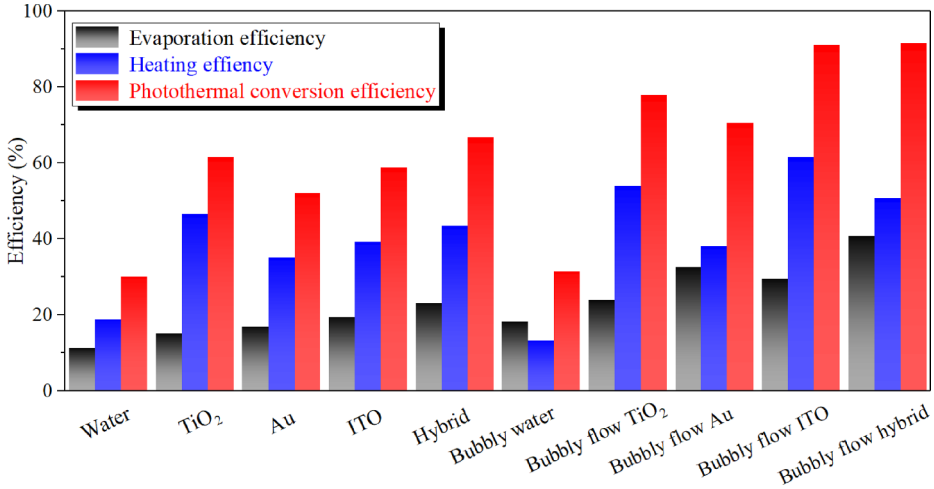

Fig. 9. Evaporation efficiency, heating and photothermal efficiency in solar evaporation of the nanofluids under one-sun.

Acknowledgements

The research was supported by grants from the Fundamental Research Funds for the Central Universities (2020DF002) and the Natural Science Foundation of China (51576002, 51806041).

References

Abd-ur-Rehman, H.M., Al-Sulaiman, F.A., 2017. A novel design of a multistage stepped bubble column humidifier for the humidification of air. Appl. Therm. Eng. 120, 530–536.

Bermel, P., Yazawa, K., Gray, J.L., Xu, X., Shakouri, A., 2016. Hybrid strategies and technologies for full spectrum solar conversion. Energy Environ. Sci. 9, 2776–2788.
Berry, K.R., Dunklin, J.R., Blake, P.A., Roper, D.K., 2015. Thermal dynamics of plasmonic nanoparticle composites. J. Phys. Chem. C. 119 (19), 10550–10557.
Chen, R., Wu, Z., Zhang, T., Yu, T., Ye, M., 2017. Magnetically recyclable self-assembled thin films for highly efficient water evaporation by interfacial solar heating. RSC Adv. 7 (32), 19849–19855.
Chen, W., Zou, C., Li, X., Liang, H., 2019. Application of recoverable carbon nanotube nanofluids in solar desalination system: an experimental investigation. Desalination 451, 92–101.
Ma, C.R., Yan, J.Y., Huang, Y.C., Wang, C.X., Yang, G.W., 2018. The optical duality of tellurium nanoparticles for broadband solar energy harvesting and efficient photothermal conversion. Sci. Adv. 4, (eaas9894).
Link, S., El-Sayed, M.A., 1999. Spectral properties and relaxation dynamics of surface plasmon electronic oscillations in gold and silver nanodots and nanorods. J. Phys. Chem. B 103, 8410–8426.
Fan, C., Shahid, M., Pashley, R.M., 2014. Studies on bubble column evaporation in various salt solutions. J. Solution Chem. 43 (8), 1297–1312.
Brewer, S., Franzen, S., 2002. Indium tin oxide plasma frequency dependence on sheet resistance and surface adlayers determined by reflectance FTIR spectroscopy. J. Appl. Phys. 106, 12986–12992.
Gao, M., Zhu, L., Peh, C.K., Ho, G.W., 2019. Solar absorber material and system designs for photothermal water vaporization towards clean water and energy production. Energy Environ. Sci. 12 (3), 841–864.
Govorov, A.O., Richardson, H.H., 2007. Generating heat with metal nanoparticles. Nano Today 2 (1), 30–38.
Ha, M., Kim, J.H., You, M., Li, Q., Fan, C., Nam, J.M., 2019. Multicomponent plasmonic nanoparticles: from heterostructured nanoparticles to colloidal composite nanostructures. Chem. Rev. 119 (24), 12208–12278.
Halas, N.J., Lal, S., Chang, W.S., Link, S., Nordlander, P., 2011. Plasmons in strongly coupled metallic nanostructures. Chem. Rev. 111 (6), 3913–3961.
Hedayati, M.K., Faupel, F., Elbahri, M., 2012. Tunable broadband plasmonic perfect absorber at visible frequency. Appl. Phys. A 109 (4), 769–773.
Hogan, N.J., Urban, A.S., Ayala-Orozco, C., Pimpinelli, A., Nordlander, P., Halas, N.J., 2014. Nanoparticles heat through light localization. Nano Lett. 14 (8), 4640–4645.
Duan, H.L., Tang, L.L., Zheng, Y., 2017. Optical properties of hybrid plasmonic nanofluid based on core_shell nanoparticles. Phys. E 91, 88–92.
Jauffred, L., Samadi, A., Klingberg, H., Bendix, P.M., Oddershede, L.B., 2019. Plasmonic heating of nanostructures. Chem. Rev. 119 (13), 8087–8130.
Jeon, J., Park, S., Lee, B.J., 2014. Optical property of blended plasmonic nanofluid based on gold nanorods. Opt. Express 22 (Suppl 4), A1101–1111.
Jeon, J., Park, S., Lee, B.J., 2016. Analysis on the performance of a flat-plate volumetric solar collector using blended plasmonic nanofluid. Sol. Energy 132, 247–256.
Jiang, N., Zhuo, X., Wang, J., 2018. Active plasmonics: principles, structures, and applications. Chem. Rev. 118 (6), 3054–3099.
Li, J.L., Wang, X.Y., Lin, Z.H., Xu, N., Li, X.Q., Liang, J., Zhao, W., Lin, R.X., Zhu, B., Liu, G.L., Zhou, L., Zhu, S.N., Zhu, L., 2020. Over 10 kg m^{-2} h^{-}1 evaporation rate enabled by a 3D interconnected porous carbon foam. Joule 4 (4), 1–10.
Langmuir, I., 1928. Oscillations in ionized gases. PNAS. 14 (8), 627–637.
Liang, J., Liu, H., Yu, J., Zhou, L., Zhu, J., 2019. Plasmon-enhanced solar vapor generation. Nanophotonics 8 (5), 771–786.
Zhou, L., Zhuang, S.D., He, C.Y., Tan, Y.L., Wang, Z.L., Zhu, J., 2017. Self-assembled spectrum selective plasmonic absorbers with tunable bandwidth for solar energy conversion. Nano Energy 32, 195–200.
Zhou, L., Tang, Y.L., Wang, J.Y., Xu, W.C., Yuan, Y., Cai, W.S., Zhu, S.N., Zhu, J., 2016. 3D self-assembly of aluminium nanoparticles for plasmon-enhanced solar desalination. Nat. Photon. 10 (6), 393–398.
Liu, C.X., Huang, J.F., Hsiung, C.-E., Tian, Y., Wang, J.J., Han, Y., Fratalocchi, A., 2017a. High-performance large-scale solar steam generation with nanolayers of reusable biomimetic banoparticles. Adv. Sustain. Syst. 1 (1–2), 1600013.
Liu, G.H., Cao, H., Xu, J.L., 2018. Solar evaporation of a hanging plasmonic droplet. Sol. Energy 170, 184–191.
Liu, G.H., Xu, J.L., Wang, K.Y., 2017b. Solar water evaporation by black photothermal sheets. Nano Energy 41, 269–284.
Loeb, S., Li, C., Kim, J.H., 2018. Solar photothermal disinfection using broadband-light absorbing gold nanoparticles and carbon black. Environ. Sci. Technol. 52 (1), 205–213.
Du, M., Tang, G.H., 2016. Plasmonic nanofluids based on gold nanorods_nanoellipsoids_nanosheets for solar energy harvestingn. Sol. Energy 137, 393–400.
Amjad, M., Raza, G., Yan, X., Pervaiz, S., Xu, J.L., Du, X.Z., Wen, D.S., 2017. Volumetric solar heating and steam generation via gold nanofluids. Appl. Energy 206, 393–400.
Ni, G., Miljkovic, N., Ghasemi, H., Huang, X., Boriskina, S.V., Lin, C.-T., Wang, J., Xu, Y., Rahman, M.M., Zhang, T., Chen, G., 2015. Volumetric solar heating of nanofluids for direct vapor generation. Nano Energy 17, 290–301.
Neumann, O., Urban, A.S., Day, J., Lal, S., Nordlander, P., Halas, N.J., 2013. Solar vapor generation enabled by nanoparticles. Acs Nano 7 (1), 42–49.
Qu, J., Zhang, R., Wang, Z., Wang, Q., 2019. Photo-thermal conversion properties of hybrid CuO-MWCNT/H_2O nanofluids for direct solar thermal energy harvest. Appl. Therm. Eng. 147, 390–398.
Ross, M.B., Blaber, M.G., Schatz, G.C., 2014. Using nanoscale and mesoscale anisotropy to engineer the optical response of three-dimensional plasmonic metamaterials. Nat. Commun. 5, 4090.
Shin, D., Kang, G., Gupta, P., Behera, S., Lee, H., Urbas, A.M., Park, W., Kim, K., 2018. Thermoplasmonic and photothermal metamaterials for solar energy applications. Adv. Opt. Mater. 6 (18), 1800317.
Tao, P., Ni, G., Song, C., Shang, W., Wu, J., Zhu, J., Chen, G., Deng, T., 2018. Solar-driven interfacial evaporation. Nature. Energy 3 (12), 1031–1041.
Verma, S.K., Tiwari, A.K., Tiwari, S., Chauhan, D.S., 2018. Performance analysis of hybrid nanofluids in flat plate solar collector as an advanced working fluid. Sol. Energy 167, 231–241.
Wang, X., He, Y., Liu, X., Shi, L., Zhu, J., 2017. Investigation of photothermal heating enabled by plasmonic nanofluids for direct solar steam generation. Sol. Energy 157, 35–46.
Wang, X.J., Wang, Y.Q., Yang, X.X., Cao, Y., 2019. Numerical simulation on the LSPR-effective core-shell copper. Sol. Energy 181, 439–451.
Yan, X., Liu, G.H., Xu, J.L., Wang, S., 2018. Plasmon heating of one-dimensional gold nanoparticle chains. Sol. Energy 173, 665–674.
Yao, G.S., Xu, J.L., Liu, G.X., 2020. Solar steam generation enabled by bubbly flow nanofluids. Sol. Energ. Mat. Sol. C. 206, 110292.
Zeiny, A., Jin, H., Lin, G., Song, P., Wen, D., 2018. Solar evaporation via nanofluids: A comparative study. Renew. Energy 122, 443–454.
Zeng, J., Xuan, Y., Duan, H., 2016. Tin-silica-silver composite nanoparticles for medium-to-high temperature volumetric absorption solar collectors. Solar Sol. Energy Mat. Sol. C 157, 930–936.